ISBN: 978-3-95450-231-8 ISSN: 2673-5490 doi: 10.18429/JACoW-IPAC2023-WEPL157

BEAM-INDUCED HEATING MITIGATION OF THE SPS KICKERS: A CRUCIAL UPGRADE TO MOVE TOWARDS HL-LHC BEAM INTENSITIES

C. Zannini*, M. Barnes, M. Diaz, L. Ducimetière, D. Standen, G. Rumolo, P. Trubacova
CERN, 1211 Geneva, Switzerland

Abstract

Beam-induced heating of equipment can have several undesirable effects, including rendering the equipment temporarily unavailable, equipment degradation and/or damage. Hence, to avoid these problems, it may be imperative to limit beam intensity. Beam-coupling impedance mitigation of existing devices and/or design optimization of new accelerator elements are essential to overcome these limitations. In this framework, a very good example is the optimization of the SPS kickers beam-coupling impedance for beam-induced heating mitigation. This paper describes the beam-coupling impedance measurements and simulation studies performed to identify and potentially remove the intensity limitation arising from the excessive beam-induced heating of an SPS injection kicker.

INTRODUCTION

The beam coupling impedance characterizes the interaction between the particle beam and an accelerator device. During the traversal through the accelerator, the particle beam will induce electromagnetic fields which will affect the motion of the beam itself. This mechanism is studied to understand, predict and prevent beam instability behaviour. However, beam induced EM fields also cause heating of the accelerator device itself. In the case of a ferrite kicker magnet, the heating resulting from the beam induced power loss [1] could raise the ferrite temperature to its Curie temperature, with risk of device damage or malfunction. It is preferable to address potential beam induced heating issues in the design phase. However, due to the more relaxed performance constraints, decades ago, beam coupling impedance effects were not systematically taken into consideration when designing new accelerator components. For this reason, the original design of the SPS ferrite loaded kickers was not optimized in terms of beam induced heating. For example, due to heating issues [2], the original design of the SPS extraction kickers (MKEs) had to be modified [3]. Interleaved fingers were printed by serigraphy directly on the ferrite. The serigraphy creates a parallel impedance that if properly engineered can shield the ferrite bringing a significant reduction of the beam coupling impedance over a broad frequency range without affecting the rise time of the kicker and its High Voltage (HV) performance [3, 4]. In the case of the SPS extraction kickers, the serigraphy brought to a significant reduction of the real part of the longitudinal impedance below 2 GHz with a consequent reduction of a factor ~4 of the beam induced heating [5, 6]. On the other hand, the serigraphy introduced an impedance resonance at 44 MHz [6]. This resonance was studied in detail and was identified to be a quarter wavelength resonance on the serigraphy fingers [5, 6]. To minimize the impact of this resonance on the beam induced heating the finger length was optimized to shift the resonance frequency as far as possible from the beam spectrum lines. This required shortening the serigraphy length by 20 mm [7]. The solution was implemented and experimentally validated during SPS scrubbing runs [8]. This solution gave an additional 40% margin in the SPS bunch intensity, which is crucial for the HL-LHC beams [9]. After the optimization of the SPS extraction kickers, the SPS injection kicker (MKP-L) became the bottleneck for CERN-SPS beam induced heating [10].

BEAM INDUCED HEATING MITIGATION OF THE SPS INJECTION KICKERS

The MKP kicker modules have C-shaped ferrite cores sandwiched between high voltage (HV) plates. Plates connected to ground are interleaved between the HV plates: the HV and ground plates form a capacitor to ground. One C-core, together with its HV and ground capacitance plates, is named a cell [11]. The kicker module is divided into 22 cells, each 31 mm long.

The SPS injection kicker system is composed of four tanks (three MKP-S and one MKP-L tank): the MKP-L tank contains four modules. The MKP-L, due to the wider aperture, has a higher impedance than the MKP-S at lower frequency. This causes a stronger interaction with the beam spectrum and hence higher beam induced power loss [12]. Figure 1 shows a comparison of the beam coupling impedance of the MKP-S and MKP-L while Fig. 2 shows the expected ratio between the MKP-L and MKP-S beam induced power loss.

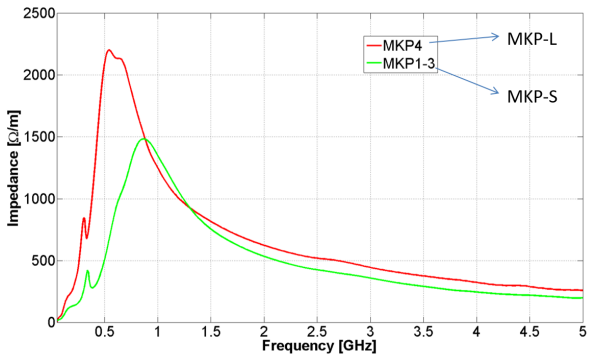

Figure 1: Real part of the longitudinal beam coupling impedance: comparison between the original MKP-L (red curve) and the MKP-S (green curve).

* carlo.zannini@cern.ch

ISBN: 978-3-95450-231-8 ISSN: 2673-5490 doi: 10.18429/JACoW-IPAC2023-WEPL157

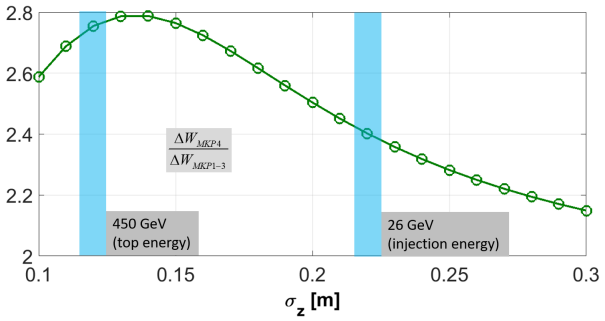

Figure 2: Power loss ratio between the original MKP-L and MKP-S as function of the bunch length.

The need to mitigate the MKP-L beam induced power loss in order to accommodate HL-LHC beam intensities was identified already in 2013 and reported in [13]. Consequently potential solutions to mitigate the beam induced heating were investigated. Based also on the SPS extraction kicker experience, a design with silver fingers was developed. However, due to the shorter length of the MKP-L ferrite cells, 31 mm in comparison with 235 mm, applying the fingers directly on an MKP-L ferrite, as done for the MKEs, was not a viable solution. It was found that significantly longer fingers, extending over several cells, would be needed to efficiently shield the impedance. This was achieved by applying silver fingers on the beam side of ceramic (Al_2O_3) plates, with the fingers connected to the module end ground plates, to ensure isolation from the ferrite and HV plates. Details about the first version of the impedance shielding of the MKP-L can be found in [14]. This initial beam coupling impedance mitigation solution was successfully verified with bench measurements (see Fig. 3).

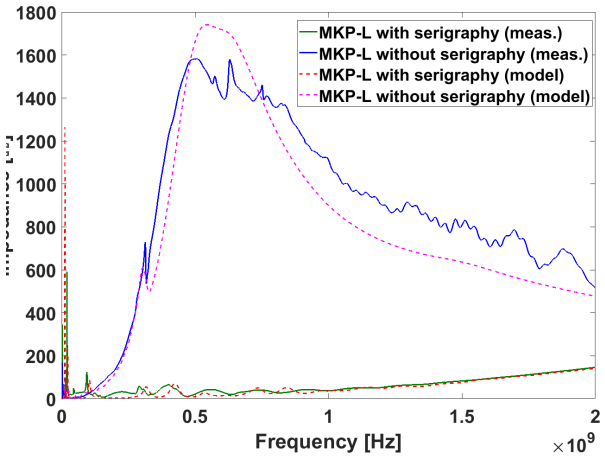

Figure 3: Real part of the longitudinal beam coupling impedance: comparison between measurements (solid lines) and simulation model (dashed lines) of the original and the new MKP-L module.

The original version (without silver fingers) of the MKP-L module, without vacuum tank, was measured using the well known stretched wire method [15]. Subsequently, the ceramic plates with fingers were inserted into the module aperture and the measurements repeated. Good agreement was observed between simulation models and measurements for both cases, with and without fingers, even showing fine details such as a small resonance, due to the cell length, at about 300 MHz. Unfortunately, this first version was not a good solution at high voltage [16]. After several investigations, the connection of the fingers to the HV end-plates was chosen as the best solution [16]. Beam coupling impedance measurements on this configuration were benchmarked against the simulation model [17]. This comparative analysis allowed a further optimization of the simulation model [17]. The improved model was used to predict the beam coupling impedance for several configurations with the silver fingers applied to Al_2O_3: Figure 4 shows a sketch of the concept. As previously mentioned, the shielding introduces an impedance resonance. The aim of the design optimization was to keep the resonance as narrow and as far as possible from high amplitude beam spectrum lines.

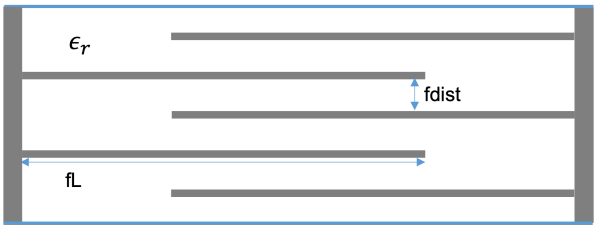

Figure 4: Sketch of the silver fingers applied to Al_2O_3.

Optimization of the MKP-L impedance shielding was needed to find the best compromise between beam induced heating mitigation and HV behavior [16]. Long fingers are required for best impedance shielding and short fingers, especially at the output end of the magnet [16], for best HV behaviour. Another relevant constraint to the impedance mitigation concerned the aperture dimensions, which limited the available ceramic thickness and gap from the ferrite cores.

Once the MKP-L design was optimized for both HV behaviour and impedance, and verified on a prototype module, all four modules were assembled [18]. A comparison between measurements and the simulation model of the fully assembled MKP-L is presented in Fig. 5. A difference of up to 2 MHz, between measurements and predictions, for the resonance near 40 MHz, occurs [19]. The slight differences between simulations and measurements are mainly related to the wire method setup which introduces an additional TEM mode and consequently additional losses [6, 20]: material properties' uncertainty is also an important factor in the model.

Figure 6 shows a comparison of the real part of the longitudinal beam coupling impedance of the original design and the new, low impedance, design. One can notice the significant reduction of the broadband impedance: however, resonances are introduced in the low frequency range. The design of the shielding has been optimized, with the HV constraints in mind, to place the dangerous

ISBN: 978-3-95450-231-8 ISSN: 2673-5490 doi: 10.18429/JACoW-IPAC2023-WEPL157

impedance resonance as far as possible from the 40 MHz, 25ns, beam spectrum line maximizing also the distance from 8b4e additional lines.

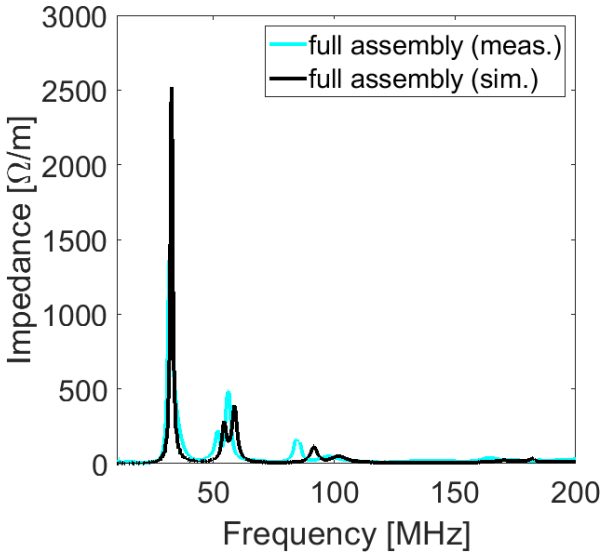

Figure 5: Real part of the longitudinal beam coupling impedance: measurements on the new MKP-L (fully assembled) and comparison with the simulation model.

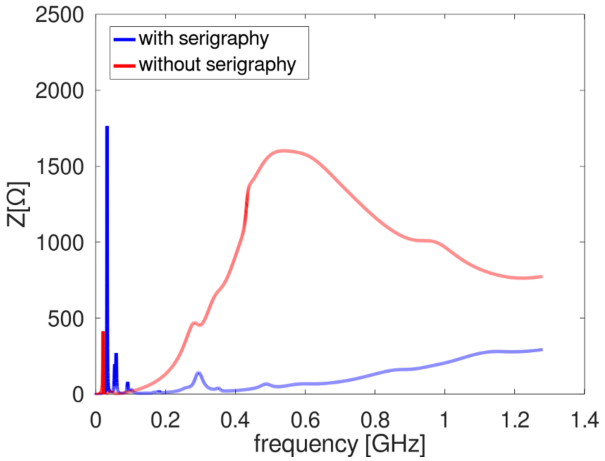

Figure 6: Real part of the longitudinal beam coupling impedance: comparison between the original and the final version of the new MKP-L module.

The low impedance MKP-L has been installed in the SPS during the Year-End Technical Stop (YETS) 2022–2023. In very good agreement with the predictions, the new MKP-L heating has been dramatically reduced and is now significantly lower than MKP-S heating. As an example, Table 1 shows a comparison of the expected power loss ratio and the measured temperature gradient ratio during the scrubbing run 2023. The relative temperature data analyzed are highlighted in Fig. 7. In agreement with the expectations, the temperature gradient ratio between MKP-S and MKP-L significantly increases during flat top scrubbing due to the reduction of the bunch length. It is also worth mentioning that, during the long flat top scrubbing, there is a high rate of change of temperature for the MKP-S, which may now be the new bottleneck in terms of beam induced heating. Long flat top scrubbing had to be adapted to allow MKP-S cooldown.

Table 1: Comparison of power loss ratio and heating ratio observed during scrubbing run 2023 for different beam types.

Beam type	$(\frac{\Delta W_{MKP-S}}{\Delta W_{MKP-L}})_{sim}$	$(\frac{\Delta T_{MKP-S}}{\Delta T_{MKP-L}})_{meas}$
flat bottom scrubbing	1.5	1.6
long flat top scrubbing	5.5	6.9
8b4e long flat top	5.2	6.3

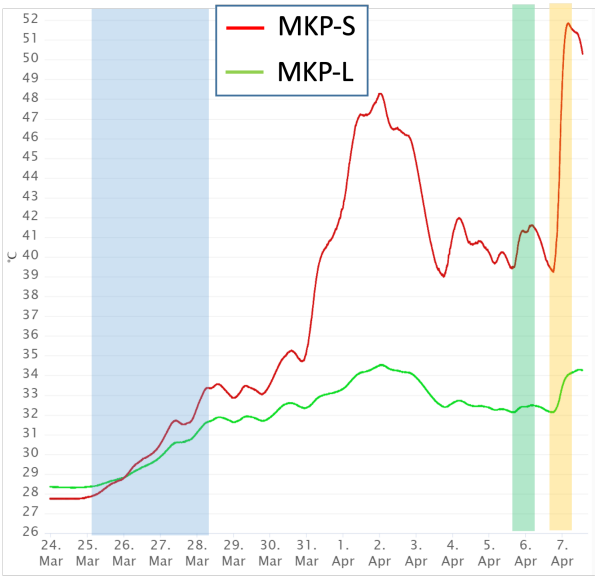

Figure 7: Temperature evolution of MKP-L and MKP-S during 2023 scrubbing run. The temperature data used in Tab. 1 have been highlighted (flat bottom scrubbing in blue, 8b4e in green and long flat top scrubbing in orange).

CONCLUSIONS

The ferrite loaded kickers are the main limitation in terms of beam induced heating in the SPS. After the optimization of the SPS extraction kickers, the bottleneck was represented by the SPS injection kickers. Due to the aperture dimensions of the MKP-L, these modules have more beam induced heating than the MKP-S. To accommodate LIU beam intensities, it was necessary to mitigate the beam induced heating of this kicker. The beam coupling impedance shielding solution of the device has been discussed. The model has been successfully validated with bench measurements. In good agreement with the expectations, the first 2023 temperature data of the new MKP-L confirm the expected effectiveness of the beam induced heating mitigation solution.

ISBN: 978-3-95450-231-8 ISSN: 2673-5490 doi: 10.18429/JACoW-IPAC2023-WEPL157

REFERENCES

[1] C. Zannini, G. Iadarola, and G. Rumolo, "Power Loss Calculation in Separated and Common Beam Chambers of the LHC," in *Proc. IPAC'14*, Dresden, Germany, Jun. 2014, pp. 1711–1713. doi:10.18429/JACoW-IPAC2014-TUPRI061

[2] M. Timmins, "SPS extraction kicker magnet: thermal analysis," CERN, Tech. Rep. TS-Note-2004-016, 2004.

[3] T. Kroyer, F. Caspers, and E. Gaxiola, "Longitudinal and Transverse Wire Measurements for the Evaluation of Impedance Reduction Measures on the MKE Extraction Kickers," CERN, Tech. Rep. CERN-AB-Note-2007-028, 2007.

[4] E. Gaxiola, J. Bertin, F. Caspers, L. Ducimetière, and T. Kroyer, "Experience with Kicker Beam Coupling Reduction Techniques," Tech. Rep. CERN-AB-2005-024, 2005.

[5] C. Zannini, "Electromagnetic Simulation of CERN accelerator components and experimental applications," CERN-THESIS-2013-076, Ph.D. dissertation, Lausanne, EPFL, 2013.

[6] C. Zannini and G. Rumolo, "EM Simulations in Beam Coupling Impedance Studies: Some Examples of Application," in *Proc. ICAP'12*, Rostock-Warnemunde, Germany, Aug. 2012, pp. 190–192. https://jacow.org/ICAP2012/papers/WESCI1.pdf

[7] C. Zannini, "Multiphysics Simulations of Impedance Effects in Accelerators," in *Proc. ICFA Mini-Workshop on Impedances and Beam Instabilities in Particle Accelerators*, Benevento, Italy, Sep. 2017, pp. 141–144. doi:10.23732/CYRCP-2018-001.141

[8] M. J. Barnes *et al.*, "Upgrading the SPS Fast Extraction Kicker Systems for HL-LHC," in *Proc. IPAC'17*, Copenhagen, Denmark, May 2017, pp. 3483–3486. doi:10.18429/JACoW-IPAC2017-WEPVA097

[9] C. Zannini *et al.*, "Low impedance design with example of kickers (including cables) and potential of metamaterials," in *Proc. MCBI 2019*, Zermatt, Switzerland, Sep. 2019, pp. 167–174. doi:10.23732/CYRCP-2020-009.167

[10] V. Kain *et al.*, "Achievements and Performance Prospects of the Upgraded LHC Injectors," in *Proc. IPAC'22*, Bangkok, Thailand, 2022, pp. 1610–1615. doi:10.18429/JACoW-IPAC2022-WEIYGD1

[11] M. Barnes, "Kicker systems," in *CERN Yellow Reports: School Proceedings*, vol. 5, 2018, pp. 229–283. doi:10.23730/CYRSP-2018-005.229

[12] C. Zannini and G. Rumolo, *MKE heating with and without serigraphy*, Presentation at the CERN SPS upgrade meeting, http://paf-spsu.web.cern.ch/paf-spsu/, 2012.

[13] J. Coupard *et al.*, "LHC Injectors Upgrade, Technical Design Report - Volume I: Protons," Tech. Rep. CERN-ACC-2014-0337, 2014, pp. 550–551. doi:10.17181/CERN.7NHR.6HGC

[14] M. S. Beck, "Simulation, measurement and mitigation of the beam induced power loss in the SPS injection kickers," CERN-THESIS-2015-374, M.S. thesis, KIT, 2015.

[15] V. G. Vaccaro, "Coupling impedance measurements: an improved wire method," INFN, Tech. Rep. INFN-TC-94-023, 1994.

[16] M. J. Barnes *et al.*, "Mitigation of High Voltage Breakdown of the Beam Screen of a CERN SPS Injection Kicker Magnet," in *Proc. IPAC'22*, Bangkok, Thailand, 2022, pp. 2868–2871. doi:10.18429/JACoW-IPAC2022-THPOTK043

[17] C. Zannini, Update on the MKPL impedance studies, Presentation at the CERN 50th IWG meeting, https://indico.cern.ch/event/1063461/, 2021.

[18] M. Barnes *et al.*, "Operational experience of a low beam coupling impedance injection kicker magnet for the CERN SPS ring," presented at IPAC'23, Venice, Italy, May 2023, paper THPA164, this conference.

[19] C. Zannini, Summary of low heating MKPL impedance studies, Presentation at the CERN 64th IWG meeting, https://indico.cern.ch/event/1206723/, 2022.

[20] M. Panniello, M. R. Masullo, and V. G. Vaccaro, "The Stretched Wire Method: A Comparative Analysis Performed by Means of the Mode Matching Technique," in *Proc. LINAC'10*, Tsukuba, Japan, Sep. 2010, pp. 932–934. https://jacow.org/LINAC2010/papers/THP081.pdf